Functional transcranial photoacoustic micro-imaging of mouse cerebrovascular cross-section and hemoglobin oxygenation changes during forepaw electrical stimulation

Lun-De Liao[a,b,1],You-Yin Chen[a,1], Chin-Teng Lin[a,b], Jyh-Yeong Chang[a], , Meng-Lin Li[c*]

[a]Department of Electrical Engineering, National Chiao Tung University, Hsinchu, 300, Taiwan

[b]Brain Research Center, National Chiao Tung University, Hsinchu, 300, Taiwan

[c]Department of Electrical Engineering, National Tsing Hua University, Hsinchu, 300, Taiwan

[1] Equal contribution.
[*]Email: mlli@ee.nthu.edu.tw

ABSTRACT

In this study, we report on using a 50-MHz functional photoacoustic microscopy (PAM) to transcranially image the cross-section and hemoglobin oxygenation (SO_2) changes of single mouse cortical vessels in response to left forepaw electrical stimulation. Three difference levels of the cortical vessels (i.e., with different-sized diameters of 350, 100 and 55 μm) on activated regions were marked to measure their functional cross-section and SO_2 changes as a function of time. Electrical stimulation of the mouse left forelimb was applied to evoke functional changes in vascular dynamics of the mouse somatosensory cortex. The applied current pulses were with a pulse frequency of 3 Hz, pulse duration of 0.2 ms, and pulse amplitude of 2 mA. The cerebrovascular cross-section changes, which indicate changes in cerebral blood volume (CBV), were probed by images acquired at 570 nm, a hemoglobin isosbestic point, while SO_2 changes were monitored by the derivatives of 560-nm images normalized to 570-nm ones. The results show that vessel diameter and SO_2 were significantly dilated and increased when compared with those of the controlled ones. In summary, the PAM shows its promise as a new imaging modality for transcranially functional quantification of single vessel diameter (i.e., CBV) and SO_2 changes without any contrast agents applied during stimulation.

Keywords: Functional imaging, photoacoustic microscopy, electrical stimulation, somatosensory cortex, vasodilatation, hemoglobin oxygenation

1. INTRODUCTION

Optical imaging has been increasingly used to study brain functions *in vivo*[1]. It provides exquisite sensitivity to hemodynamic changes either via intrinsic contrast in absorption and scattering, or extrinsic contrast[2]. Diffusion optical imaging (DOI)[3] and laser speckle imaging (LSI)[4] techniques have been widely used for in vivo optical imaging of the cerebral hemodynamic changes. The DOI technique directly acquires cerebral-blood-volume (CBV), oxy-hemoglobin (HbO_2) and deoxy-hemoglobin (Hb) changes noninvasively in response to electrical stimulation of rat forepaw through intact skull[3]. However, its reconstructed images suffer from poor spatial resolution due to the diffusive nature of light in biological tissue[5]**.** LSI superficially probes the vasomotion and blood-flow responses to electrical stimulation in rat peripheral trigeminal system with high resolution (~6.7 × 6.7 μm) under a thinned skull preparation[4] Nevertheless, only superficial information can be probed by the LSI technique since its penetration depth and depth resolution are poor even with a thinned skull (Miao et al., 2010).

Photoacoustic (PA) imaging is a hybrid imaging technique that combines the advantages of both optics and ultrasound – namely, high optical absorption contrast and ultrasonic spatial resolution up to a penetration depth of ~5 cm [6]. A pulsed laser in the visible or near-infrared (NIR) range is used to irradiate a biological sample, and absorption of

Photons Plus Ultrasound: Imaging and Sensing 2011, edited by Alexander A. Oraevsky, Lihong V. Wang,
Proc. of SPIE Vol. 7899, 78992X · © 2011 SPIE · CCC code: 1605-7422/11/$18 · doi: 10.1117/12.874449

pulsed laser energy by biological tissue induces PA waves via thermoelastic effect. The distribution of optical absorption in a sample can be reconstructed by using PA signals acquired through a highly-sensitive ultrasound receivers. By taking advantage of the ultrasonic detection and reconstruction, PA imaging can provide sub-millimeter spatial resolution which is better than DOI. Recently, Maslov et al. has developed a reflection-mode confocal PA-microscopic (PAM) imaging technique with dark field illumination and a high-frequency (> 20 MHz) ultrasound transducer, being able to provide high spatial resolution around 15 μm with a penetration depth up to 3 mm[7]. We have applied such a micro-imaging technique to detect relative functional changes in CBV and hemoglobin oxygen saturation (SO2) in cerebral vessels of rats during the stimulation[8]. By leveraging distinct absorption spectra of oxy- and deoxy-hemoglobin, we demonstrated the PAM's capability of imaging hemodynamic changes in an activated region in exposed rodent brain in vivo.

In this study, we applied a functional photoacoustic micro-imaging technique to investigate peripheral stimulus-evoked changes in vessel diameter (i.e., CBV) and SO_2 in single cortical vessels with skull intact. Forepaw electrical stimulation was employed to repeatedly evoke neuronal activation in the primary somatosensory cortex. The selected vessels on activated region were marked to monitor the hemodynamic changes. The correlation between the electrical stimulation paradigms with the corresponding changes in each single vessel was discussed. Results showed that fPAM reliably probes changes in CBV and SO_2 in single cortical vessels by using intrinsic optical-absorption contrast. This technique complements other existing neuro-imaging approaches for investigating the coupling between neuronal activation and hemodynamic responses of single cerebral vessels.

2. MATERIALS AND METHODS

2.1 50-MHz Dark field confocal functional photoacoustic microscopy system

In this study, a 50-MHz dark field confocal fPAM system was used to image functional changes in cortical vessels transcranially. An optical parametric oscillator (Surlite OPO Plus, Continuum, USA) pumped by a frequency-tripled Nd:YAG Q-switched laser (Surlite II-10, Continuum, USA) was employed to provide ~4ns laser pulses at a pulse repetition rate of 10 Hz. Because in the visible spectral range, blood owns strong optical absorption and thus generates strong PA signals, laser pulses at two visible wavelengths – 560 and 570 nm (λ_{560} and λ_{570}) – were used for PA wave excitation, instead of NIR. The two wavelengths were optimized to provide high signal-to-noise ratio and sensitivity to probe functional changes in CBV and SO_2 in blood vessels[8]. In addition, to enable transcranial imaging capability, a large numerical-aperture, wideband 50-MHz ultrasonic transducer was typically used, which allows efficient collection of transcranial PA signals from cortical vessels[9]. This transducer had a -6dB fractional bandwidth of 57.5%, a focal length of 9 mm and a 6-mm active element.

Laser energy was delivered by a 1-mm multimode fiber. The fiber tip was coaxially aligned with a convex lens, an axicon, a plexiglass mirror, and the ultrasonic transducer on an optical bench, forming dark field illumination confocal with the focal point of the ultrasonic transducer. The incident energy density on the sample surface was well within the ANSI safety limit of 20 mJ/cm^2. The transducer was immersed in an acrylic water tank during the imaging process, with a hole at the bottom sealed with a piece of 15-μm thick polyethylene film. The mouse head was coated with a thin layer of ultrasonic gel, and attached to the thin film to ensure good coupling of transcranial PA waves to the tank. The PA signals received by the ultrasonic transducer were pre-amplified by a low-noise amplifier (AU-3A-0110, Miteq, USA), cascaded to an ultrasonic receiver (5073 PR, Olympus, USA), then digitized and sampled by a computer-based 14-bit analog to digital (A/D) card (CompuScope 14200, GaGe, USA) at 200-MHz sampling rate for data storage. Fluctuations of the laser energy were monitored by a photodiode (DET36A/M, Thorlabs, USA). The recorded photodiode signals were applied to compensate for PA signal variations caused by laser-energy instability before any further signal processing. Currently, the used fPAM had a 3-mm penetration depth, and the signal-to-noise ratio (SNR) at the depth of 3 mm is about 18 dB where the SNR is defined as the ratio of the signal peak value to the root-mean-square value of the noise. The maximum achievable spatial (for B-scan) and temporal resolution (for A-line) of the current fPAM is 36 μm in axial, 65 μm in lateral and 100 ms, respectively. Note that the PA images in this study were acquired without any signal averaging to facilitate the imaging of fast hemodynamic response, and the amplitudes of the envelope-detected PA signals were used in the following functional imaging analysis.

2.2 Experimental animals

Six male BALB/cByJNarl mice (National Laboratory Animal Center, Taiwan), weighing 25 - 28 grams, were used. The animals were housed at a constant temperature and humidity with free access to food and water. Before imaging experiments, the mice fasted for 24 hours but were given water ad libitum. All animal experiments were

conducted in accordance with guidelines from Animal Research Committee of National Chiao-Tung University and National Tsing Hua University. Mice were initially anesthetized by intraperitoneal injection of ketamine (91 mg/kg) and xylaxine (9.1 mg/kg). Supplemental α-chloralose (25 mg/kg/h) anesthesia was administered intraperitoneally as needed. Body temperature was maintained with 150-watt bulb heating. Anesthetized animal were mounted on the custom-made acrylic stereotaxic head holder, and the scalp was surgically removed from the skull to expose the bregma landmark. Then the exposed skull was cleaned with 0.9% sodium chloride irrigation solution right before imaging. The ultrasonic gel was applied for ultrasound coupling and maintaining skull hydration. The anteroposterior (AP) distance between the bregma and the interaural line was directly surveyed. The bregma was 3.8 ± 0.12 mm (mean ± standard deviation [SD]; n = 6) anterior to the interaural line. The animal's head was positioned in a stereotaxic frame. After the mouse was secured to the stereotaxic frame and placed on the bed pallet, the pallet was moved until the crosshair of the laser alignment system pointed out at the bregma, and then positioned in the fPAM system. The interaural and bregma references were then used to position the heads in the fPAM system. There was no additional surgery in the following experiments.

2.3 Forepaw electrical stimulation

Forepaw stimulation was achieved by insertion of thin needle stainless electrodes under the skin of the left forepaw. Electrical stimulation provided with a stimulator (Model 2100, A-M Systems, USA) consisted of a monophasic constant current at 2-mA pulses with 0.2 ms pulse-width at a frequency of 3 Hz. For functional signal acquisitions, a block design paradigm was employed in this study. Each trail consisted of three blocks, each block started with a 20-second baseline, followed by 5-second stimulation-ON and 75-second stimulation-OFF. There was a 5 seconds lapse between the blocks. PA B-scan images were acquired in each blocks to assess for stimulation-induced functional changes in selected single vessels.

2.4 Functional PA imaging

According to our previous work[8], the two used wavelengths (i.e., λ_{560} and λ_{570}) were optimal for sensing changes in CBV, SO_2 and total hemoglobin concentration, providing high signal-to-noise ratio and sensitivity to probe *in vivo* functional changes in blood vessels. At λ_{570}, an isosbestic point of the molar extinction spectra of oxy- and deoxy-hemoglobin, the optical absorption is insensitive to the SO_2 level. That is, PA signal changes at λ_{570} dominantly resulted from changes in total hemoglobin concentration. The CBV changes can be probed by the cross-sectional changes of the PA B-scan images of the cross-sections of the selected vessels at λ_{570}. In addition, the largest absorption changes occur approximately at λ_{560} in the visible spectral range when the SO_2 level changes, indicating that PA signal changes at λ_{560} are sensitive to SO2 changes. Therefore, in this study, PA signals/images at λ_{570} were used to probe the changes in CBV and HbT. To observe the SO_2 level changes only, excluding effects of HbT changes, PA signals/images acquired at λ_{560} was normalized by that acquired at λ_{570} on a pixel-by-pixel basis. Reference images ($I_{R(570)}$) at λ_{570} for a stimulation-OFF ($I_{R\,(570),\,stimulation\text{-}OFF}$) and a stimulation-ON ($I_{R(570),\,stimulation\text{-}ON}$) block were acquired. For the same region, respective images ($I_{(560)}$) at λ_{560} for stimulation-OFF ($I_{(560),\,stimulation\text{-}OFF}$) and stimulation-ON ($I_{(560),\,stimulation\text{-}ON}$) blocks were also acquired. Functional images ($\Delta I_{F(560)}$) were then constructed according to the following equation:

$$\begin{aligned}\Delta I_{F(560)} &= \frac{I_{(560\text{ nm})stimulation-ON}}{I_{R(570\text{ nm})stimulation-ON}} - \frac{I_{(560\text{ nm})stimulation-OFF}}{I_{R(570\text{ nm})stimulation-OFF}} \\ &= I_{F(560)stimulation-ON} - I_{F(560)stimulation-OFF},\end{aligned} \tag{1}$$

Note that negative values in $\Delta I_{F(560)}$ (i.e., a positive in $-\Delta I_{F(560)}$) indicated increases in SO_2 levels, and vice versa[8].

3. EXPERIMENTAL RESULTS

3.1 Transcranial imaging of mouse cerebral vasculatures

The cerebral cortex vasculature with skull intact was imaged *in vivo* by C-scan imaging of fPAM at λ_{570} (see Fig. 1). Some branches of arterioles from middle cerebral artery (MCA) vessels system can be seen in the projected C-scan image. The superior sagittal sinus (SSS) and increasing branching levels of bilateral arterioles from MCA (MI and MII) with respect to the vessels sizes of 350, 100 and 55 μm in the projected C-scan image were used to trace the functional changes in CBV and SO_2. Note that SSS images obtained by the current fPAM were not satisfactory; the imaging results were similar to those obtained in the literature[8]. The geometric focus and the finite detection bandwidth of the ultrasound transducer used may be accounted for the weakness of the detected PA signals from the SSS.

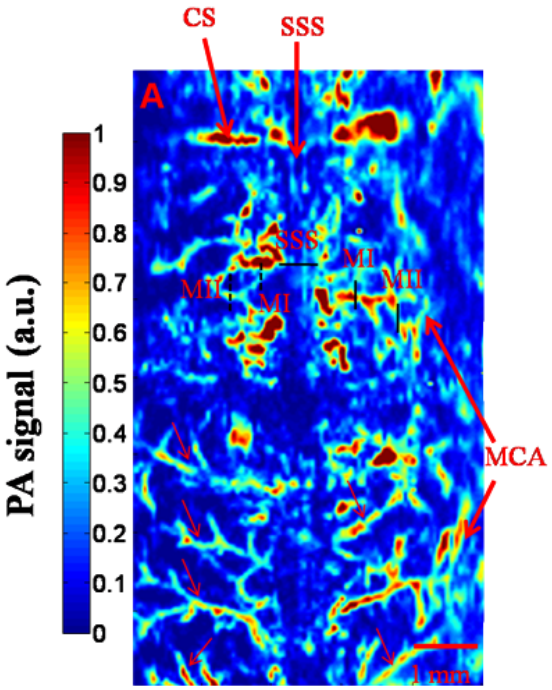

Fig. 1 *In vivo* PA-projected C-scan image of the blood vessels in the superficial layer of the cortex with skull intact, acquired at λ_{570}. The superior sagittal sinus (SSS), coronal suture (CS) and middle cerebral artery (MCA) on the cortical surface could be identified. Functional B-scan images were acquired by scanning along the black solid and dashed lines for the bilateral region, which were SSS, bilateral MI and MII arterioles with respect to about 350, 100 and 55 μm vessels sizes, respectively. The bilateral MI arterioles were cross-through the anatomical borders of the primary motor cortex and secondary motor cortex. The bilateral MII arterioles were located in the anatomical borders of the primary somatosensory cortex for the forepaw (S1FL).

3.2 Cross-sectional area (CBV) changes in SSS, bilateral MI and MII arterioles under stimulus-OFF and stimulus-ON conditions

The time-course B-scan images of vascular cross-sectional changes (i.e., CBV changes) of SSS and bilateral MI and MII arterioles for the stimulation-OFF and stimulation-ON conditions are shown in Fig. 2. Note that these images are acquired atλ_{570}. The time of peak CBV changes is 7.92 seconds for contralateral MI arteriole and 18.3 seconds in contralateral MII artery after the stimulation onset. The peak CBV ratio changes in the contralateral MI and MII arterioles comparing with the baseline are 1.160 ± 0.005% ($p < 0.0001$) and 1.270 ± 0.004% ($p < 0.001$), respectively (paired *t*-test; $n = 6$). In contrast, on the ipsilateral side, both MI and MII arterioles show no significant changes comparing with the baseline during stimulation ($p > 0.05$). Also, no significant CBV ratio changes are found in SSS

during stimulation ($p > 0.05$). The response time of CBV ratio changes from the Stimulation-ON and then return to the baseline is 13.32 seconds for contralateral MI artery and 18.43 seconds for contralateral MII artery.

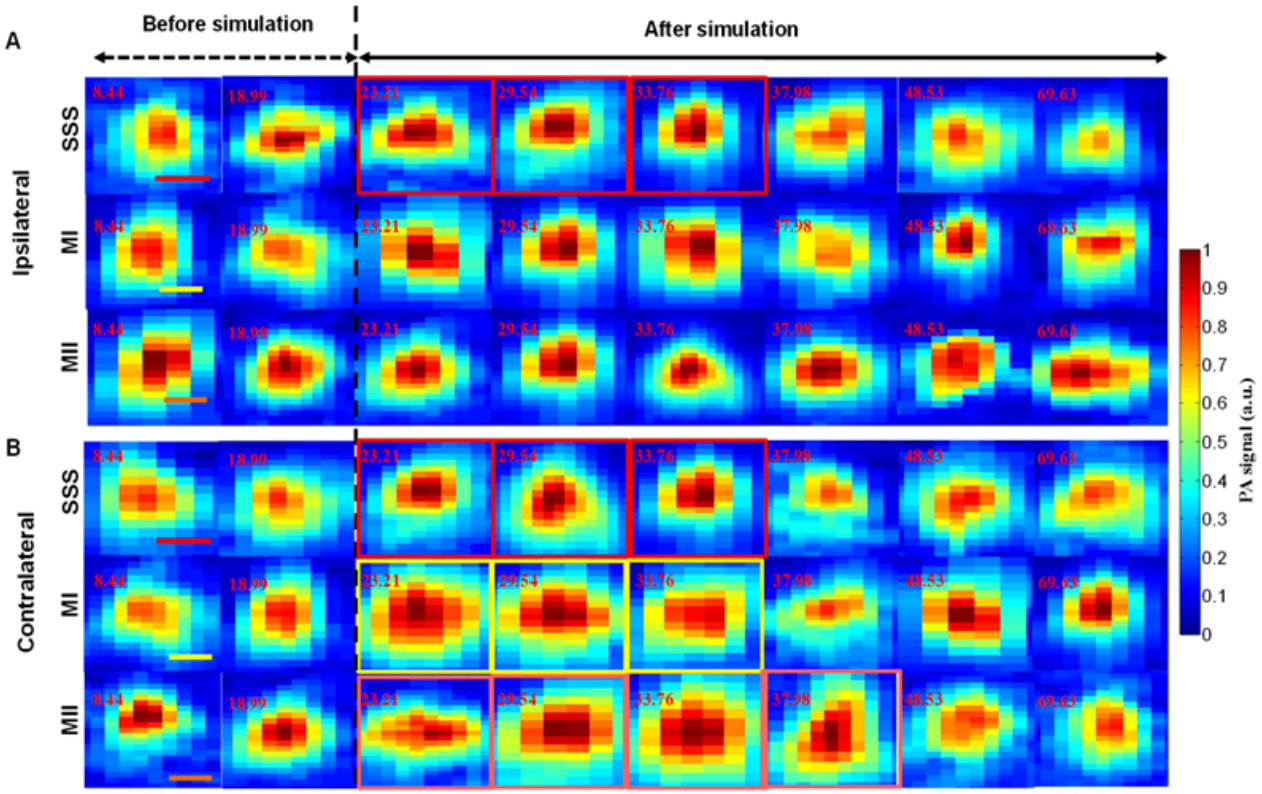

Fig. 2 *In vivo* PA B-scan images at λ_{570} of the cross-sectional area of the SSS and bilateral MI and MII arterioles from stimulation-OFF to stimulation-ON. Significant CBV changes in SSS, contralateral MI and MII arterioles were marked by the square lines in red, yellow and orange color during time series, respectively. The visualized B-scan images indicate that no significant CBV (i.e., cross-section) changes in ipsilateral MI and MII arterioles during the stimulation period. A: ipsilateral; B: contralateral.

3.3 SO_2 changes in SSS, bilateral MI and MII arterioles under stimulus-OFF and stimulus-ON conditions

The $\Delta I_{F(560)}$ signals are used to probe SO_2 changes in SSS, bilateral MI, and MII arterioles. The negative values in $\Delta I_{F(560)}$ (i.e., a decrease in $I_{F(560)}$) indicated increases in SO_2 levels, and vice versa. The SO_2 changes of B-scan images at 29.54, 23.52 and 34.77 seconds staring from the first point of Stimulation-OFF are shown in Fig. 3 for the SSS and bilateral MI and MI arterioles. These visualized images show the more significant changes of SO_2 in contralateral MI and MII than those in the ipsilateral side. The SO_2 change in SSS is also significant comparing to the baseline. The time of peak SO_2 changes are 9.54, 13.52 and 14.77 seconds for the SSS and contralateral MI and MII arterioles after the stimulation onset. The peak values of SO_2 changes comparing with the baseline image were 2.510 ± 0.001% ($p < 0.001$) in contralateral MI and 3.480 ± 0.008% ($p < 0.001$) in MII arterioles during stimulation (Wilcoxon matched-pairs signed-rank test, $n = 6$). The observed peak SO_2 increase in SSS is 1.170 ± 0.005% ($p < 0.001$) during stimulation (Wilcoxon matched-pairs signed-rank test, $n = 6$). No significant changes are observed in the ipsilateral MI and MII arterioles from Stimulation-ON to Stimulation-OFF ($p > 0.05$). The response time of SO_2 changes staring from

the Stimulation-ON and then returning to the baseline is 27.76, 21.52 and 23.79 seconds for SSS, contralateral MI and MII arterioles, respectively.

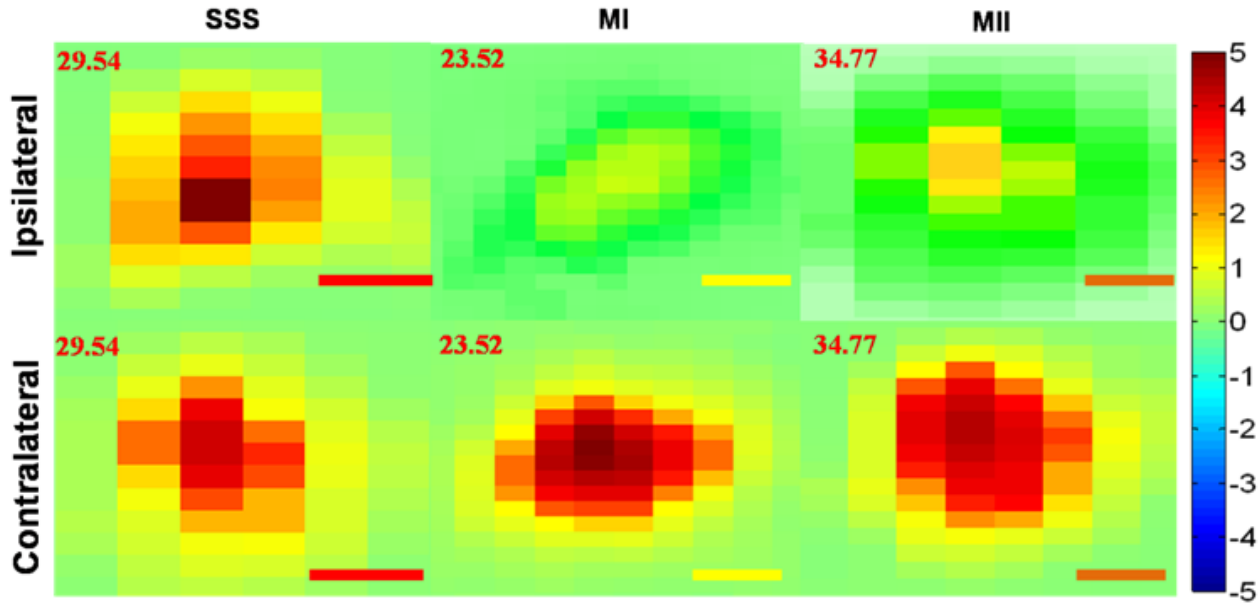

Fig. 3 $-\Delta I_{F(560)}$ PA images of the cross-sections of the SSS and bilateral MI and MII arterioles acquired at 29.54, 23.52 and 34.77 seconds, respectively.

4. CONCLUSIONS

In summary, the present study demonstrated the unique feature of a novel fPAM system in characterizing the hemodynamic response in single vessels transcranially. Local CBV and SO2 changes to forepaw electrical stimulation can be simultaneously recorded in single vessels with 36 × 65 μm of spatial resolution. The fPAM technique explored here shows its promise in understanding neurovascular coupling and elucidating the physiological basis of other imaging techniques such as fMRI approaches.

ACKNOWLEDGEMENTS

We are greatly indebted to the National Science Council, Taiwan for the support of this research through shares in grants Nos. NSC 97-2221-E-007-084-MY3, NSC96-2220-E-009-029 and NSC 97-2220-E-009-029, and funding support from National Tsing Hua University (Boost program 98N2531E1) and Ministry of Education, Taiwan..

REFERENCES

[1] E. M. C. Hillman, "Optical brain imaging in vivo: techniques and applications from animal to man", Journal of Biomedical Optics 12, 051402 (2007)
[2] D. Malonek and A. Grinvald, "Interactions between electrical activity and cortical microcirculation revealed by imaging spectroscopy : implications for functional brain mapping" Science 272, 551 (1996)
[3] J. P. Culver et al., "Evidence that cerebral blood volume can provide brain activation maps with better spatial resolution than deoxygenated hemoglobin", NeuroImage 27, 947 (2005)
[4] N. Li et al, "High spatiotemporal resolution imaging of the neurovascular response to electrical stimulation of rat peripheral trigeminal nerve as revealed by in vivo temporal laser speckle contrast", Journal of Neuroscience Methods 176, 230 (2009)

[5] H. Dehghani, S. Srinivasan, B. W. Pogue, and A. Gibson, “Numerical modelling and image reconstruction in diffuse optical tomography”, Philosophical Transactions of the Royal Society A: Mathematical, Physical and Engineering Sciences 367, 3073 (2009)
[6] L. V. Wang,” Multiscale photoacoustic microscopy and computed tomography”, Nature Photonics 3, 503 (2009)
[7] K. Maslov, G. Stoica, and L. V. Wang, “In vivo dark-field reflection-mode photoacoustic microscopy,” Optics Letter 30, 625 (2005)
[8] L.-D. Liao et al, “Imaging brain hemodynamic changes during rat forepaw electrical stimulation using functional photoacoustic microscopy”, NeuroImage 52, 562 (2010)
[9] E. W. Stein, K. Maslov, and L. V. Wang, “Noninvasive, in vivo imaging of blood-oxygenation dynamics within the mouse brain using photoacoustic microscopy”, Journal of Biomedical Optics 14, 020502 (2009)